

# Efficient retrieval of vegetation leaf area index and canopy clumping factor from satellite data to support pollutant deposition assessments

Ned Nikolov<sup>a,\*</sup>, Karl Zeller<sup>b,1</sup>

<sup>a</sup> *Natural Resource Research Center, 2150 Centre Avenue, Building A, Room 368, Fort Collins, CO 80526, USA*

<sup>b</sup> *USDA FS Rocky Mountain Research Station, 240 W. Prospect Road, Fort Collins, CO 80526, USA*

Received 25 March 2005; accepted 19 August 2005

*The paper presents a physics-based algorithm for retrieval of vegetation LAI and canopy-clumping factor from satellite data to assist research of pollutant deposition and trace-gas exchange. The method is employed to derive a monthly LAI dataset for the conterminous USA and verified at a continental scale.*

## Abstract

Canopy leaf area index (LAI) is an important structural parameter of the vegetation controlling pollutant uptake by terrestrial ecosystems. This paper presents a computationally efficient algorithm for retrieval of vegetation LAI and canopy clumping factor from satellite data using observed Simple Ratios (SR) of near-infrared to red reflectance. The method employs numerical inversion of a physics-based analytical canopy radiative transfer model that simulates the bi-directional reflectance distribution function (BRDF). The algorithm is independent of ecosystem type. The method is applied to 1-km resolution AVHRR satellite images to retrieve a geo-referenced data set of monthly LAI values for the conterminous USA. Satellite-based LAI estimates are compared against independent ground LAI measurements over a range of ecosystem types. Verification results suggest that the new algorithm represents a viable approach to LAI retrieval at continental scale, and can facilitate spatially explicit studies of regional pollutant deposition and trace gas exchange.

© 2005 Elsevier Ltd. All rights reserved.

**Keywords:** Leaf area index; Canopy density; Clumping factor; LAI data set; Seasonal LAI; Vegetation remote sensing; Reflectance model; Retrieval algorithm; Land surface property; Vegetation patchiness

## 1. Introduction

Canopy leaf area index (LAI) is typically defined as the one-sided area of green foliage projected onto a unit area of ground. As a measure of vegetation density LAI is normally expressed in units of  $\text{m}^2 \text{m}^{-2}$ . Since green foliage is the primary organ of plant photosynthesis and transpiration, LAI is an important structural parameter of vegetation canopies controlling the exchange of energy and trace gases (including pollutants) between terrestrial ecosystems and the atmosphere (e.g.

Bonan, 1991a,b; Amthor, 1994; Nemani and Running, 1996; Guenther et al., 1995; Liu et al., 1997; Hunt et al., 1996; King et al., 1997; Waring et al., 1998; Nikolov and Zeller, 2003). Thus, LAI is critical in estimating terrestrial carbon sequestration, net primary production, hydrologic watershed budgets, and pollutant deposition (e.g. Zeller and Nikolov, 2000). Landscape distribution of LAI is also considered to be important in predicting meso-scale weather circulation due to the impact of vegetation on the partitioning of incoming solar energy into latent and sensible heat fluxes (Pielke et al., 1998; Eastman et al., 2001a,b; Lu et al., 2001; Pielke, 2001).

Although direct measurements of LAI are available at many locations throughout the world (e.g. Scurlock et al., 2001), such observations are insufficient to infer the large-scale distribution and temporal dynamics of this critical canopy parameter.

\* Corresponding author. Tel.: +1 970 980 3303.

E-mail addresses: [nnikolov@fs.fed.us](mailto:nnikolov@fs.fed.us), [ntconsulting@comcast.net](mailto:ntconsulting@comcast.net) (N. Nikolov), [kzeller@fs.fed.us](mailto:kzeller@fs.fed.us) (K. Zeller).

<sup>1</sup> Tel.: +1 970 498 1238.

Current biophysical, atmospheric, and pollutant deposition models require spatially continuous fields of LAI and its seasonal variation that can be feasibly retrieved only from remotely sensed satellite data. Several global data sets of satellite-derived LAI have been proposed over the past decade (e.g. Sellers et al., 1996; Hunt et al., 1996; Nemani and Running, 1996; Myneni et al., 1997, 2002). Some of the early data sets feature a relatively coarse spatial resolution ranging from  $0.25^\circ$  (ca. 25 km) to  $1^\circ$  (ca. 100 km). They have been derived from spectral vegetation indices (SVI) such as the Normalized Difference Vegetation Index (NDVI) or the Greenness Index (GI), also known as Simple Ratio (SR) of near-infrared to red reflectance. These methods employed empirical/statistical relationships between LAI and SVIs that do not account for bi-directional optical effects. While these relationships work well under a particular viewing and illumination geometry, they produce inaccurate results when applied over the broad range of optical geometrical conditions normally encountered in satellite images. This is because the interpretation of an SVI in terms of LAI strongly depends on sensor view angle, solar elevation, and sun-sensor relative azimuth. At spatial resolutions of 1-km or finer, topography (i.e. pixel slope and aspect) also needs consideration as it begins to impact the apparent viewing and illumination conditions.

The importance of bi-directional corrections of spectral reflectances for vegetation parameter retrieval has been well documented in both modeling and field studies (e.g. Qi et al., 1995; Gastellu-Etchegorry et al., 1999; Leroy and Hauteceur, 1999; Bicheron and Leroy, 1999). There are three basic types of BRDF models – physics-based, empirical, and semi-empirical. It is now recognized that reliable estimation of LAI from remotely sensed data requires implementation of physics-based canopy radiative transfer models that provide realistic simulation of the bi-directional reflectance distribution function (BRDF). Recently, Knyazikhin et al. (1998a,b) proposed a synergistic algorithm for LAI retrieval based on a detailed 3-D radiative transfer model that accounts for all known bi-directional effects. Due to its complexity, the model could not be directly inverted to solve for LAI. Instead, a look-up table (LUT) was generated from numerous solutions of the radiative model for different LAI values and under various viewing and illumination conditions and background (soil) albedos. The algorithm retrieves canopy LAI from satellite data by comparing measured multispectral reflectances with model solutions stored in the LUT. The method is currently operationally employed with MODIS data to retrieve global LAI fields (Myneni et al., 2002; Tian et al., 2002a,b). This is the first attempt to employ a BRDF model in LAI remote sensing at the global scale. However, the synergistic algorithm of Knyazikhin et al. (1998a,b) has a potential drawback. It retrieves canopy LAI by matching the measured reflectance field in numerous spectral bands to a multispectral solution in the LUT. If no successful match is found, the algorithm resorts to biome-specific empirical relationships between LAI and NDVI that do not account for BRDF effects. According to Myneni et al. (2002), the LUT fails to provide a solution, and the algorithm switches to the empirical functions in about

50% of cases in broadleaf and conifer forests. This introduces uncertainty into the final LAI product because not all pixel values are estimated by the same numerical technique.

In this paper, we present a new simple and computationally efficient method for the retrieval of canopy LAI and foliage-clumping factor from satellite images based on a *direct* numerical inversion of an analytical BRDF model. The method interprets the SR spectral vegetation index (also known as Greenness Index, GI) while accounting for major effects of viewing and illumination geometry on bi-directional reflectances in the red and near-infrared band induced by topography, and the position of the Sun and the satellite sensor. The algorithm never fails to deliver a solution within the range of illumination and viewing conditions typically found in satellite data. This ensures a consistency among the LAI estimates of all pixels in the final product. Unlike other physics-based methods, this algorithm does *not* require computationally intensive inversion techniques. The feasibility of the method is demonstrated with 1-km resolution AVHRR data from 1995 employed to retrieve monthly LAI maps of the conterminous USA.

## 2. LAI retrieval algorithm

The new LAI retrieval method is based on an analytical solution to the multiple scattering equation of Ross (1981) proposed by Camillo (1987). The canopy spectral reflectances  $I_d(u)$  and  $I_f(u)$  in direction  $u$  due to scatter of the direct solar beam (d) and the incoming diffuse radiation (f) are given by

$$I_d(u) = A_1 \frac{1 + a_0 u}{1 - k_0 u} + B_1 \frac{1 - a_0 u}{1 + k_0 u} + h_0 \frac{1 + b_0 u}{1 + K u} + h_1 \frac{\sqrt{1 - u^2}}{1 + K u} \cos(\Delta\phi) \quad (1)$$

$$I_f(u) = A_0 \frac{1 + a_0 u}{1 - k_0 u} + B_0 \frac{1 - a_0 u}{1 + k_0 u} \quad (2)$$

where  $I_d(u)$  and  $I_f(u)$  are expressed in decimal fractions,  $u = \cos \theta_{\text{sat}}$  ( $\theta_{\text{sat}}$  is the satellite/sensor zenith angle),  $K$  is the canopy light-extinction coefficient for direct solar radiation,  $\Delta\phi$  is the solar relative azimuth, while coefficients  $A_1$ ,  $B_1$ ,  $A_0$ ,  $B_0$ ,  $a_0$ ,  $b_0$ ,  $k_0$ ,  $h_0$ , and  $h_1$  are non-linear functions of solar elevation, sensor zenith angle, relative azimuth, leaf optical properties (i.e. reflectance and transmittance), background/soil albedo, and total stand LAI. These functions are derived from equations and radiation boundary conditions documented by Camillo (1987). Camillo verified the analytical solution (i.e. Eqs. (1) and (2)) against canopy reflectance measurements taken over different crop fields at various viewing angles and solar elevations. The model was shown to reproduce observed data within the measurement error.

The current retrieval algorithm computes the direct-beam extinction coefficient ( $K$ ) as a function of solar elevation and the canopy mean leaf inclination angle ( $\theta$ ) using the ellipsoidal leaf angle distribution model by Campbell (1986), i.e.

$$K = \frac{G(u_o)}{u_o} = \frac{[u_o^2(\chi^2 - 1) + 1]^{0.5}}{u_o[\chi + 1.744(\chi + 1.182)^{-0.733}]} \quad (3)$$

here,  $G(u_o)$  is the ratio of projected to total leaf area in direction  $u_o = \cos \theta_{\text{sun}}$  (where  $\theta_{\text{sun}}$  is the solar zenith angle),  $\chi$  is the ratio of vertical to horizontal projection of a representative volume of foliage. For canopies with spherical leaf angle distribution  $\chi = 1$ , for planophile canopies  $\chi > 1$ , and for erectophile canopies  $\chi < 1$ . The algorithm estimates  $\chi$  as a function of the canopy mean leaf inclination angle ( $\Theta$ ) following Wang and Jarvis (1988), i.e.

$$\chi = \begin{cases} 151.515 \frac{1 - 0.0107\Theta}{\Theta} & \text{if } \Theta \geq 57.4^\circ \\ 97.087 \frac{1 - 0.0053\Theta}{\Theta} & \text{if } \Theta < 57.4^\circ \end{cases} \quad (4)$$

Eq. (4) is an empirical fit to results from a numerical integration of Campbell's ellipsoidal angle density function (Campbell, 1990). For spherical canopies  $\Theta = 57.4^\circ$ , for planophile canopies  $0^\circ < \Theta < 57.4^\circ$ , and for erectophile canopies  $57.4^\circ < \Theta < 90^\circ$ .

The physical realism of Camillo's radiative transfer model was further improved through several modifications. (1) A foliage-clumping factor ( $\Omega$ ) was introduced into the equations for computing coefficients  $A_1$  through  $h_1$ . Foliage-clumping measures the degree of aggregation of individual leaves into shoots, tree crowns and vegetation patches. Clumping increases light penetration into the canopy. As a result, the effective leaf area index  $L_e$  (i.e. LAI seen by the incident radiation) is always smaller than the actual LAI ( $L_t$ ). In mathematical terms,  $L_e = \Omega L_t$  where  $0 < \Omega \leq 1$ . A small  $\Omega$  indicates a greater degree of clumping. In real vegetation stands,  $\Omega$  typically ranges between 0.50 and 0.97 (e.g. Chen, 1996; Chen et al., 2003). Analysis of data on light attenuation in forest canopies reported by Sampson and Smith (1993) and Chen (1996) suggests that  $\Omega$  declines exponentially with total LAI according to the formula:

$$\Omega = 0.492\{1 + \exp[-0.52(L_t - 0.45)]\} \quad (5)$$

This function was incorporated into the reflectance model to convert reflectance-based estimates of effective LAI into ones of actual LAI. (2) The average canopy leaf inclination angle ( $\Theta$ ) was made dependent on stand LAI. Based on unpublished data by Nikolov, it was assumed that  $\Theta$  gradually declines from  $75^\circ$  at  $L_t = 0.25$  to  $39^\circ$  at  $L_t = 6.0$  according to the formula:

$$\Theta = 26.0\{1 + \exp[-0.26(L_t - 3.1)]\} \quad (6)$$

Since  $\Theta = 57.4^\circ$  corresponds to a spherical leaf angle distribution (Campbell, 1990), this function implies that, as stand LAI increases, leaf orientation changes from predominantly erectophile to spherical to primarily planophil. (3) The background (soil) reflectance was made a function of viewing direction and solar elevation by incorporating the anisotropic soil reflectance model (SOILSPECT) of Jacquemoud et al. (1992) as parameterized by Privette et al. (1995). A

non-Lambertian soil reflectance is important for accurately estimating LAI of thin/sparse canopies, where background reflectance significantly influences the outgoing radiative fluxes at the canopy top. (4) Effects of topography (e.g. pixel slope and aspect) on the apparent sensor view angle and solar elevation were incorporated into the canopy reflectance model. Pixel slope and orientation were derived from the USGS 30-s (ca. 1-km) GTOPO30 data set using IDRISI GIS. This improved the LAI retrieval in mountainous regions.

The total canopy reflectance  $\rho_i(u)$  in direction  $u$ , where subscript  $i$  denotes either red (r) or near-infrared (nir) spectral band, is estimated as a weighted sum of the reflectances resulting from the scatter of the incident direct ( $Q_d$ ) and diffuse ( $Q_f$ ) irradiances, i.e.

$$\rho_i(u) = \frac{Q_d I_d(u) + Q_f I_f(u)}{Q_d + Q_f} \quad (7)$$

The partitioning of incident solar radiation into diffuse and direct components is calculated as a function of pixel mean altitude, slope, and aspect using equations by Erbs et al. (1982), and Yang and Miller (1995). Slope and aspect (i.e. slope orientation) are also used to calculate the apparent viewing and illumination angle for each map pixel, and to correct the direction  $u = \cos \theta_{\text{sat}}$ . Terrain adjustments of satellite-reported view and solar angles are made using equations of 3-D incident radiation geometry discussed by Nikolov and Zeller (1992).

Finally, a directional Greenness Index is calculated by the model as a ratio of near-infrared to red canopy reflectance, i.e.

$$GI = \frac{\rho_{\text{nir}}(u)}{\rho_{\text{r}}(u)} \quad (8)$$

Vegetation LAI is estimated from satellite-measured GIs and reported viewing- and illumination-geometry data by inverting the above reflectance algorithm. This is accomplished using an iterative binary search technique, where  $L_t$  is progressively adjusted from an initial LAI value until modeled GI matches the observed GI with an accuracy of  $\pm 0.01$ . The initial LAI value is set to  $4.0 \text{ m}^2 \text{ m}^{-2}$  if the observed GI is greater than 7.0 or to  $2.0 \text{ m}^2 \text{ m}^{-2}$  if  $GI < 7.0$ . The algorithm uses eight input data layers to produce a single LAI map, i.e.

- Reflectance in the red band,
- Reflectance in the near-infrared band,
- Satellite zenith view angle,
- Solar zenith altitude angle,
- Sun-sensor relative azimuth,
- Terrain elevation,
- Terrain slope,
- Terrain aspect (slope orientation).

Table 1 lists all input parameters required by the LAI retrieval model. The spectral optical characteristics of green foliage and soils (i.e. background) were fixed to theoretically

Table 1  
Input parameters of the LAI retrieval model

Parameter	Units	Typical range/value
Greenness Index (a ratio of measured near-infrared to red reflectance)	Dimensionless	$0.5 < GI < 30.0$
Solar zenith angle	Degree	$0^\circ < \theta_{\text{sun}} < 70^\circ$
Satellite view angle	Degree	$0^\circ < \theta_{\text{sat}} < 50^\circ$
Sun-sensor relative azimuth angle	Degree	$0^\circ < \Delta\Phi < 180^\circ$
Terrain slope	Degree	$0 < s < 30$
Terrain aspect	Degree	$0 < a < 360$
Terrain elevation	Meter	$0 < z < 8848$
Leaf red reflectance	Decimal fraction	$\rho_r = 0.075$
Leaf red transmittance	Decimal fraction	$\tau_r = 0.064$
Leaf NIR reflectance	Decimal fraction	$\rho_{\text{nir}} = 0.50$
Leaf NIR transmittance	Decimal fraction	$\tau_r = 0.39$
Soil/background albedo in the red	Decimal fraction	$\alpha_r = 0.25$
Soil/background albedo in the NIR	Decimal fraction	$\alpha_{\text{nir}} = 0.33$

representative values. The intent behind this approach was to make the algorithm independent of vegetation type, and, thus, more generic and easy to apply at continental and global scales. Fig. 1 depicts variations in the functional relationship between GI and LAI simulated by the improved canopy reflectance model (discussed above) using parameter values from Table 1. A model sensitivity analysis suggested that the sensor view angle has by far the largest impact on the GI–LAI relationship among all optical geometry factors. Therefore, correcting SVIs for directional viewing effects is critical to a successful LAI retrieval.

### 3. Retrieval of 1-km resolution data sets of canopy LAI and clumping factor for the conterminous USA

The above algorithm was applied to 10-day composite AVHRR images from 1995 in combination with the GTOPO30 elevation data set (<http://edcdaac.usgs.gov/gtopo30/gtopo30.html>) to retrieve monthly maps of vegetation LAI and foliage-clumping factor for the conterminous USA. The USGS Global Land 1-km AVHRR Project (<http://edcdaac.usgs.gov/1KM/1kmhomepage.html>) provided the required satellite data layers. The product was derived using a three-step approach:

- (1) LAI maps were estimated for each 10-day composite period of the AVHRR data set from January through December 1995 employing the above LAI retrieval algorithm.
- (2) A maximum LAI map was constructed for every month of 1995 by selecting the highest predicted LAI value for each pixel out of three estimates obtained in that month. This procedure aims to reduce the effect of cloud contamination on the LAI estimates. Presence of clouds tends to underestimate LAI since radiation absorption of water vapor is stronger in the near-infrared band than it is in the red. The result was a series of 12 digital LAI maps composed

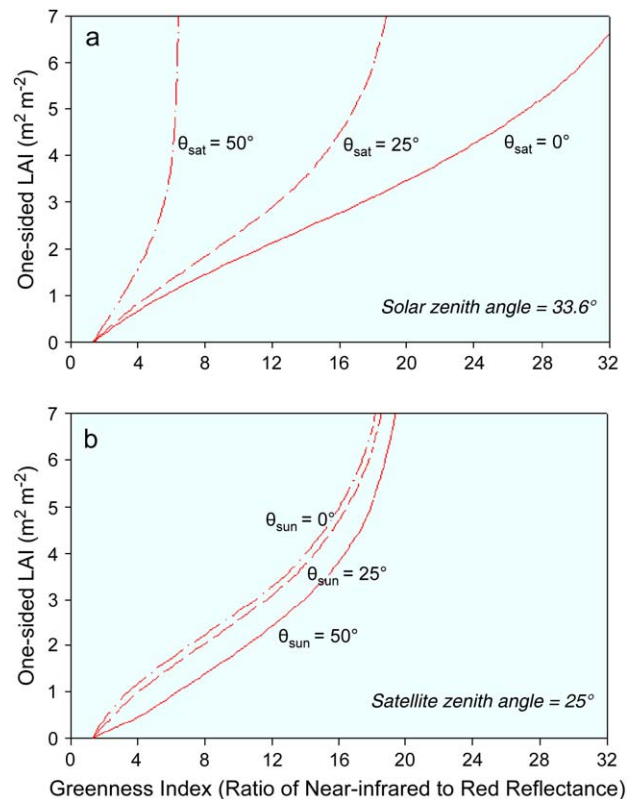


Fig. 1. Variation of the relationship between canopy LAI and Greenness Index as a function of (a) sensor view zenith angle ( $\theta_{\text{sat}}$ ), and (b) solar zenith angle ( $\theta_{\text{sun}}$ ) simulated by the BRDF retrieval model used in this study.

of pixels displaying canopy development on different days in each month.

- (3) The ‘raw’ LAI data set produced in Step 2 was further processed to smooth temporal variations in predicted canopy densities (caused by residual cloud contamination and occasional missing data), and to interpolate LAI values, so that all pixels of a monthly map refer to day 15 of that month. Smoothing of the seasonal LAI variation was done on a pixel basis using an algorithm that eliminates anomalous values from the temporal sequence. Detection of anomalous values was based on the assumption that seasonal variations of LAI do not exhibit rapid upward–downward fluctuations over consecutive months. A rational-function interpolation (Press et al., 1988) was applied to the remaining monthly data points of each pixel to calculate canopy LAI for day 15 in each month of 1995. Finally, the newly interpolated monthly LAI maps were saved into a data set.

The foliage-clumping index was computed from a composite map of peak-seasonal LAI using Eq. (5). Fig. 2 illustrates the seasonal LAI data set for the conterminous USA by portraying maps of vegetation density for four months of 1995. Fig. 3 depicts spatial patterns of peak summer LAI and the foliage-clumping factor for the Western USA. Figs. 4 and 5 illustrate the retrieved summer-maximum LAI over regions of the US West and East Coast, respectively.

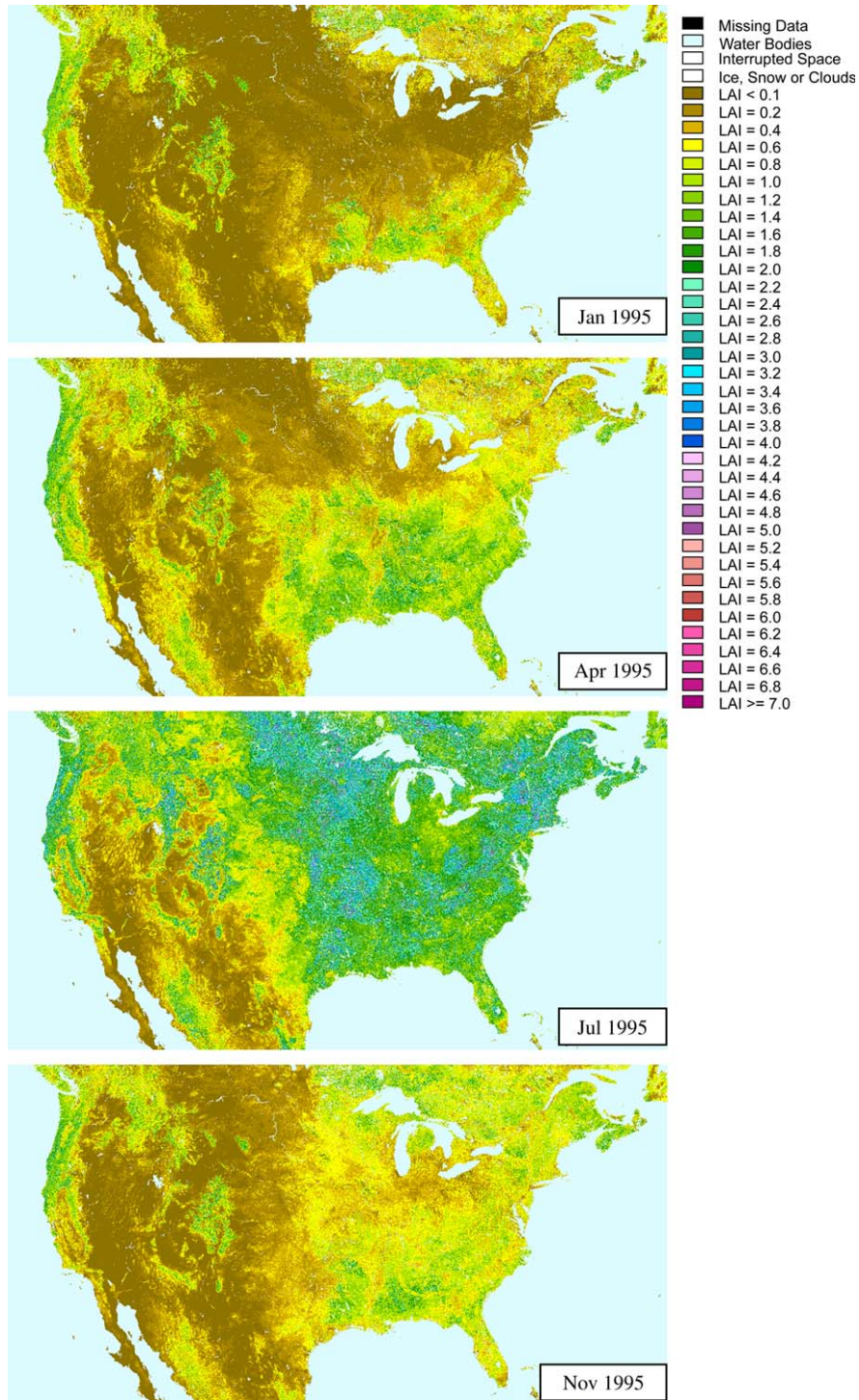


Fig. 2. Seasonal changes of vegetation LAI over the conterminous USA retrieved from 1-km resolution AVHRR data.

#### 4. LAI product validation

Verification of satellite-based LAI estimates is not trivial. It requires carefully designed field measurements that meet several criteria: (1) sample plots on the ground must be sufficient in number and allocated in a way that yields a representative LAI average for each map pixel being verified. This is particularly important for satellite-derived LAI estimates of 1-km or

coarser resolution. (2) The uncertainty of the employed LAI measurement method must be known to properly assess errors in the LAI retrievals. (3) Field measurements should be conducted at approximately the same time (i.e. day of year) when satellite images used to retrieve LAI information were acquired. This ensures that verification results are not affected by time-dependent differences in vegetation growth and/or phenology. (4) LAI field measurements should represent

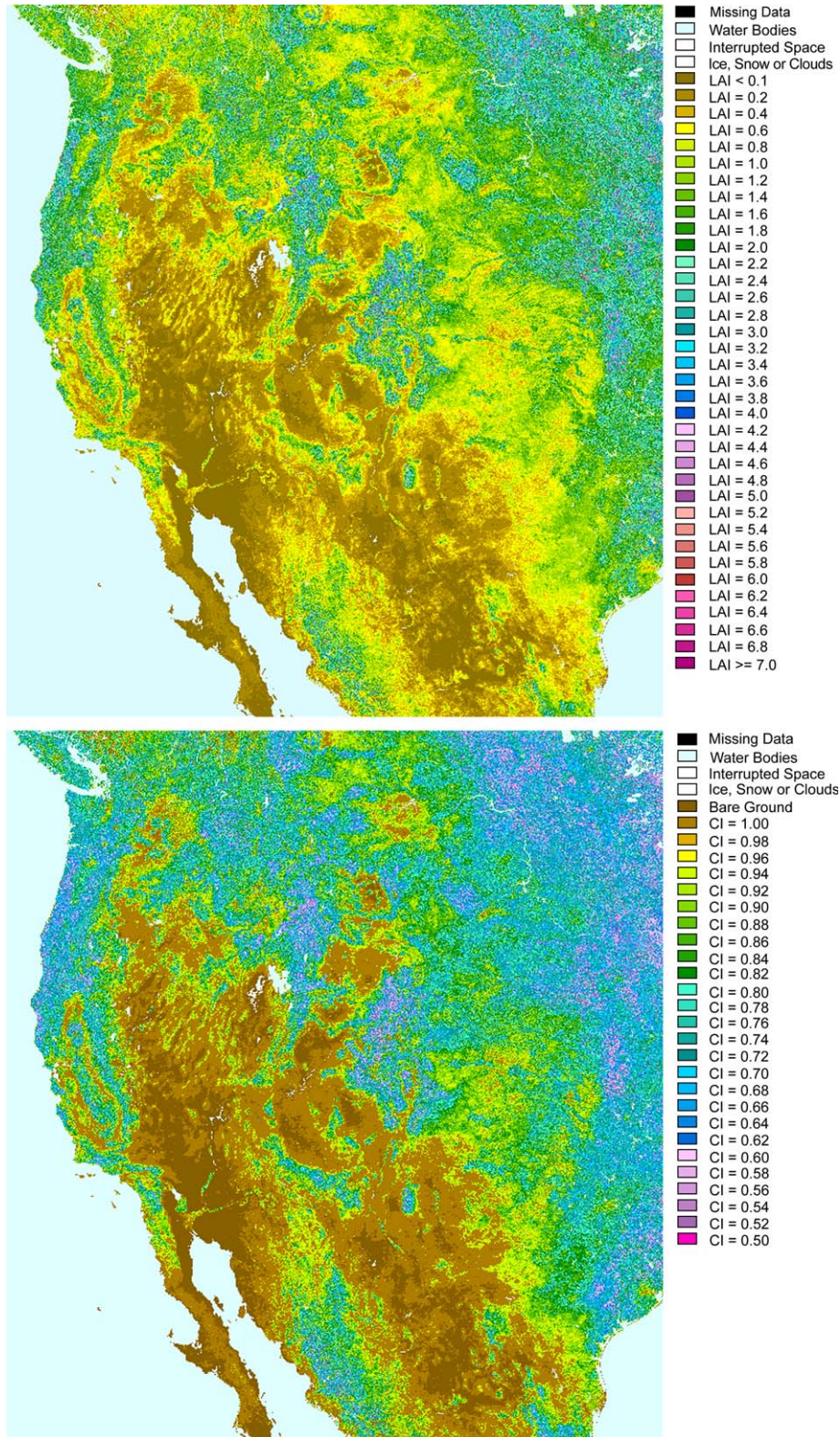


Fig. 3. Peak summer LAI (upper panel), and canopy foliage-clumping index (CI) (lower panel) over the Western USA retrieved from 1-km resolution AVHRR data.

a broad range of vegetation types and canopy densities to enable verification of the retrieval algorithm under a variety of conditions.

It is not common that a validation data set meets all of the above criteria. Therefore, satellite-derived LAI maps are

seldom fully verifiable. With this in mind, we attempted a partial validation of the new LAI product using independent ground measurements of vegetation density reported by Scurlock et al. (2001) and Karlik (2002). Scurlock et al. (2001) compiled a database of 1008 LAI observations from

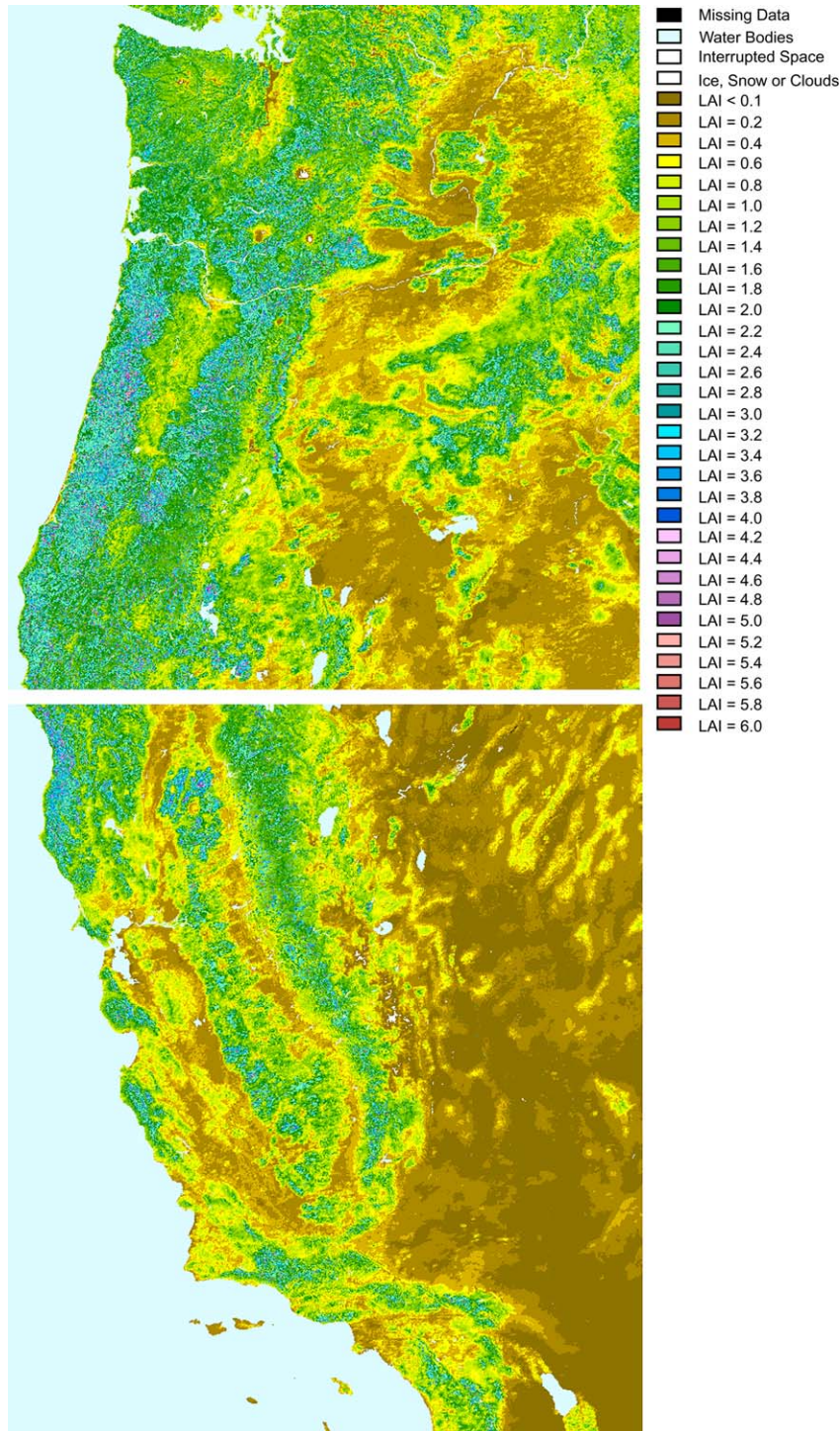


Fig. 4. Peak summer LAI over Oregon and Washington states (upper) and California and Nevada (lower) retrieved from 1-km AVHRR data.

nearly 400 unique field studies conducted worldwide from 1932 to 2000 using over 300 original-source references. The database is available online at the ORNL DAAC ([http://www-eosdis.ornl.gov/VEGETATION/lai\\_des.html](http://www-eosdis.ornl.gov/VEGETATION/lai_des.html)). We obtained 77 LAI observations from the data set for 18 locations within the conterminous USA between 1991 and 1999. Measurements represented eight biomes dominated by over 22 deciduous and coniferous species (see Table 2). At each

location defined by latitude and longitude, multiple LAI measurements (when available) were averaged to yield a representative LAI value that was then compared to the satellite-derived peak summer LAI estimate for that location.

Karlik (2002) reported LAI measurements for Central California as part of a field study aimed to validate various vegetation databases for modeling of biogenic emissions. The study was funded by the California Air Resources Board

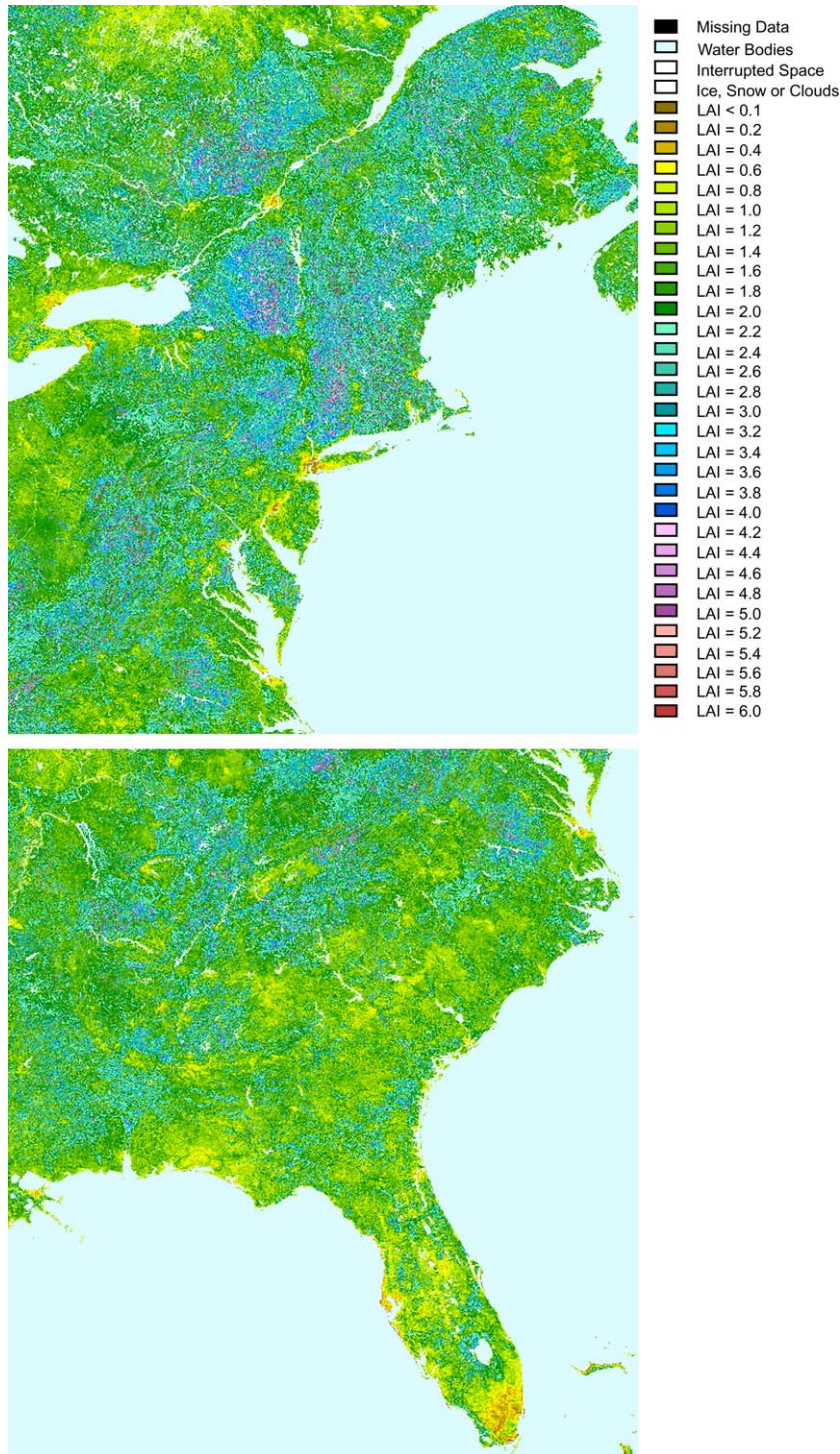


Fig. 5. Peak summer LAI over Northeastern (upper) and Southeastern (lower) USA retrieved from 1-km AVHRR data.

and EPA, and implemented by the University of California Cooperative Extension at Berkeley (CA). LAI observations were made in the summer of 1999 in an oak-savannah ecosystem using LAI-2000 (Li-Cor, Inc) and CI-110 (CID, Inc) instruments. Karlik (2002) compared vegetation density measurements at 12 sample plots (along a canopy gradient) with retrieved summer LAI values from the 1-km data set. We used results from his analysis in our validation exercise.

Fig. 6 portrays a scatter plot of observed vs. satellite-derived LAI data for all measurement locations reported by Scurlock et al. (2001) and Karlik (2002) in Table 2. Regression statistics indicated a very good agreement between the two data sets, e.g.  $r^2 = 0.96$ , Slope = 0.94 and Intercept =  $-0.06$  (Slope and Intercept are not significantly different from 1.0 and 0.0, respectively, at the 0.05 probability level, i.e.  $P_{\text{slope}} = 0.12$ ,  $P_{\text{intercept}} = 0.63$ ). This suggests a satisfactory

Table 2  
Characteristics of the LAI measurement sites in USA used to validate the satellite-derived LAI product in this study

Latitude	Longitude	Number of plots	Measured LAI	Retrieved LAI	Year measured	Biome type	Dominant species
46.17	–89.67	4	5.40	5.0	1992	Evergreen, needle leaf	<i>Pinus resinosa</i>
46.10	–89.50	11	3.10	3.00	1992	Deciduous, broadleaf	<i>Populus, Acer, Quercus</i>
46.00	–88.90	2	6.95	6.6	1992	Deciduous, broadleaf	<i>Acer, Tsuga</i>
45.90	–90.20	5	4.88	4.4	1992	Deciduous, broadleaf	<i>Acer, Tilia, Fraxinus</i>
44.75	–124.00	2	5.55	5.8	1994	Deciduous, broadleaf	<i>Alnus rubra</i>
44.68	–110.55	4	0.49	0.4	1997	Sub-alpine forest	<i>Pinus contorta</i>
44.50	–123.5	1	6.30	6.4	1994	Evergreen, needle leaf	<i>Pseudotsuga menziesii</i>
44.25	–121.75	1	0.8	0.8	1994	Evergreen, needle leaf	<i>Pinus ponderosa</i>
44.25	–122.00	1	3.00	2.8	1994	Evergreen, needle leaf	<i>Tsuga mertensiana</i>
44.00	–121.50	1	0.40	0.6	1994	Woodland	<i>Juniperus occidentalis</i>
43.87	–91.85	10	6.68	6.6	1993	Deciduous, broadleaf	<i>Quercus rubra</i>
39.92	–107.38	6	5.68	5.6	1991	Evergreen, needle leaf	<i>Picea engelmannii</i>
38.94	–86.37	3	3.40	3.0	1993	Mixed Hardwood Forest	<i>Quercus prinus</i>
37.40	–122.22	8	1.04	1.0	1996	Crops	<i>Helianthus annuus</i>
36.60	–119.50	1	3.29	2.6	1992	Orchard	<i>Juglans regia</i>
35.00	–79.00	12	1.66	1.4	1995	Evergreen, needle leaf	<i>Pinus taeda</i>
33.10	–83.42	1	3.90	4.0	1994	Pine forest	<i>Pinus taeda</i>
41.37	–106.24	4	2.80	2.4	1996	Sub-alpine forest	<i>Picea engelmannii</i>
Central CA	Central CA	12	1.44	1.2	1999	Oak-Savannah	<i>Quercus, Salix, Prunus</i>

See Fig. 6 for a statistical comparison between retrieved and measured LAI values. LAI observations are from Scurlock et al. (2001) and Karlik (2002).

accuracy of the LAI retrieval algorithm. Such validation results are particularly encouraging in view of the fact that: (1) sample plots were smaller than a square kilometer (i.e. the size of an LAI map pixel) and, thus, may not have adequately represented the mean vegetation density over the target area; (2) in most cases, LAI measurements were made several years apart from the time of satellite image acquisition, which may have introduced a bias to the comparison caused by disturbance history and/or variations in weather conditions; and (3) most studies did not quantify the statistical uncertainty of LAI measurements making it difficult to assess the true error in the LAI retrievals. Since this verification involves

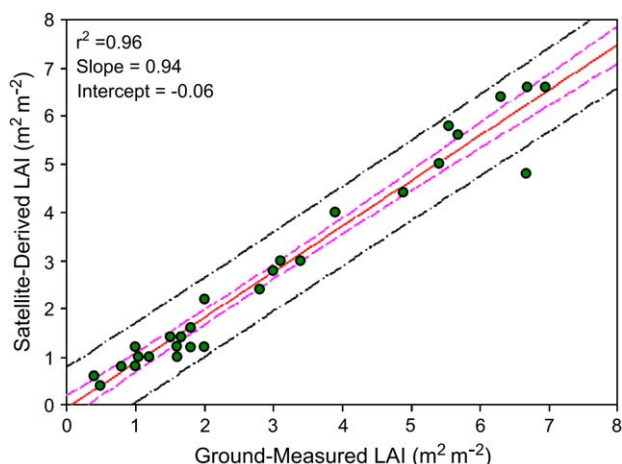


Fig. 6. Comparison of 1-km resolution LAI estimates retrieved from 1995 AVHRR satellite data with LAI ground measurements in the USA obtained from 1991 to 1999. The dash line shows the 95% confidence interval. The dash-dotted line indicates the prediction intervals. Slope and Intercept are not significantly different from 1.0 to 0.0, respectively, at the 0.05 probability level. Most LAI observations are from a worldwide LAI database compiled by Scurlock et al. (2001) (Oak Ridge National Laboratory, Oak Ridge, TN). Karlik (2002) provided some LAI measurements for Central California. See Table 2 for details.

canopy measurements from a variety of ecosystems and vegetation types, the results indicate a robustness of the new LAI retrieval algorithm.

## 5. Conclusion

We presented a simple and efficient algorithm for canopy LAI retrieval based on interpretation of satellite-measured directional Simple Ratio vegetation indices. The method uses numerical inversion of an analytical one-dimensional canopy radiative transfer model that accounts for major effects of viewing and illumination geometry on bi-directional reflectances. Results from application of the algorithm to 1-km resolution AVHRR satellite data suggest that:

- Satellite-based spectral vegetation indices such as SR and NDVI need to be corrected for effects of sensor view angle, solar elevation, and topography before used for canopy LAI retrieval.
- Vegetation density can be reliably retrieved at a continental scale from remotely sensed data without a detailed knowledge of vegetation type and ecosystem-specific soil reflectance characteristics if a physics-based radiative transfer model is employed.
- The new retrieval algorithm is suitable for application with regional studies of pollutant deposition and atmosphere–ecosystem trace gas exchange.

## Acknowledgements

The Air Resources Program of the USFS Rocky Mountain Research Station (RMRS) in Fort Collins, CO funded the development of the LAI data set. The USFS Pacific Southwest Research Station (PSWRS) in Riverside, CA provided

invaluable logistical support to the project. N and T Services LLC, a consulting company in Fort Collins, CO, executed the project. The authors express their deep gratitude to R. Fisher from FS RMRS, Dr. M. Arbaugh, Dr. A. Bytnerowicz and Mrs. R. Orly from FS PSWRS, and Dr. J. Pederson from the California Air Resources Board Research Division in Sacramento, CA for their guidance, support, and professional cooperation.

## References

- Amthor, J.S., 1994. Scaling CO<sub>2</sub>-photosynthesis relationships from the leaf to the canopy. *Photosynth. Res.* 39 (3), 321–350.
- Bicheron, P., Leroy, M., 1999. A method of biophysical parameter retrieval at global scale by inversion of a vegetation reflectance model. *Remote Sens. Environ.* 67, 251–266.
- Bonan, G.B., 1991a. A biophysical surface energy budget analysis of soil temperature in the boreal forests of interior Alaska. *Water Resour. Res.* 27, 767–781.
- Bonan, G.B., 1991b. Atmosphere–biosphere exchange of carbon dioxide in boreal forests. *J. Geophys. Res.* 96, 7301–7312.
- Camillo, P., 1987. A canopy reflectance model based on an analytical solution to the multiple scattering equation. *Remote Sens. Environ.* 23, 453–477.
- Campbell, G.S., 1990. Derivation of an angle density function for canopies with ellipsoidal leaf angle distributions. *Agric. For. Meteorol.* 49, 173–176.
- Campbell, G.S., 1986. Extinction coefficient for radiation in plant canopies calculated using an ellipsoidal inclination angle distribution. *Agric. For. Meteorol.* 36, 317–321.
- Chen, J.M., Liu, J., Leblanc, S.G., Lacaze, R., Roujean, J.-L., 2003. Multi-angular optical remote sensing for assessing vegetation structure and carbon absorption. *Remote Sens. Environ.* 84, 516–525.
- Chen, J.M., 1996. Optically-based methods for measuring seasonal variation of leaf area index in boreal conifer stands. *Agric. For. Meteorol.* 80, 135–163.
- Eastman, J.L., Coughenour, M.B., Pielke Sr., R.A., 2001a. The regional effects of CO<sub>2</sub> and landscape change using coupled plant and meteorological model. *Global Change Biol.* 7, 797–815.
- Eastman, J.L., Coughenour, M.B., Pielke Sr., R.A., 2001b. Does grazing affect regional climate? *J. Hydrometeorol.* 2, 243–253.
- Erbs, D.G., Klein, S.A., Duffie, J.A., 1982. Estimation of the diffuse radiation fraction for hourly, daily, and monthly-average global radiation. *Sol. Energy* 28, 293–302.
- Gastellu-Etchegorry, J.P., Guillevic, P., Zagolski, F., Demarez, V., Trichon, V., Deering, D., Leroy, M., 1999. Modeling BRDF and radiation regime of boreal and tropical forests: I. BRDF. *Remote Sens. Environ.* 68, 281–316.
- Guenther, A., Hewitt, C.N., Erickson, D., Fall, R., Geron, C., Graedel, T., Harley, P., Klinger, L., Lerdau, M., McKay, W.A., Pierce, T., Scholes, B., Steinbrecher, R., Tallamraju, R., Taylor, J., Zimmerman, P., 1995. A global model of natural volatile organic-compound emissions. *J. Geophys. Res. Atmos.* 100 (D5), 8873–8892.
- Hunt Jr., E.R., Piper, S.C., Nemani, R., Keeling, C.D., Otto, R.D., Running, S.W., 1996. Global net carbon exchange and intra-annual atmospheric CO<sub>2</sub> concentrations predicted by an ecosystem process model and three-dimensional atmospheric transport model. *Global Biogeochem. Cycles* 10 (3), 431–456.
- Jacquemoud, S., Baret, F., Hanocq, J.F., 1992. Modeling spectral bidirectional soil reflectance. *Remote Sens. Environ.* 41, 123–132.
- Karlik, J.F., 2002. Validation of Databases for Modeling Biogenic Volatile Organic Compound Emissions in Central California (Final Report No. 00-16CCOS). University of California Cooperative Extension, Bakersfield, CA, 99 pp.
- King, A.W., Wullschleger, S.D., Post, W.M., 1997. Seasonal biosphere–atmosphere CO<sub>2</sub> exchange and terrestrial ecosystem carbon storage: mechanism, extrapolation, and implications. In: *Extended Abstracts of Fifth International Carbon Dioxide Conference*. Cairns, Queensland, Australia, pp. 257–258.
- Knyazikhin, Y., Martonchik, J.V., Diner, D.J., Myneni, R.B., Verstraete, M., Pinty, B., Gobron, N., 1998a. Estimation of vegetation leaf area index and fraction of absorbed photosynthetically active radiation from atmosphere-corrected MISR data. *J. Geophys. Res.* 103, 32239–32256.
- Knyazikhin, Y., Martonchik, J.V., Myneni, R.B., Diner, D.J., Running, S.W., 1998b. Synergistic algorithm for estimating vegetation canopy leaf area index and fraction of absorbed photosynthetically active radiation from MODIS and MISR data. *J. Geophys. Res.* 103, 32257–32274.
- Leroy, M., Hautecoeur, O., 1999. Anisotropy-corrected vegetation indices derived from POLDER/ADEOS. *IEEE Trans. Geosci. Remote Sens.* 37 (3), 1698–1708.
- Liu, J., Chen, J.M., Chihlar, J., Park, W.M., 1997. A process-based boreal ecosystem productivity simulator using remote sensing inputs. *Remote Sens. Environ.* 62, 158–175.
- Lu, L., Pielke Sr., R.A., Liston, G., Parton, W.J., Ojima, D., Hartman, M., 2001. Implementation of a two-way interactive atmospheric and ecological model and its application to the central United States. *J. Clim.* 14, 900–919.
- Myneni, R.B., Hoffman, S., Knyazikhin, Y., Privette, J.L., Glassy, J., Tian, Y., Wang, Y., Song, Y., Smith, G.R., Lotsch, A., Friedl, M., Morisette, J.T., Votava, P., Nemani, R.R., Running, S.W., 2002. Global products of vegetation leaf area and fraction absorbed PAR from year one of MODIS data. *Remote Sens. Environ.* 83, 214–231.
- Myneni, R.B., Nemani, R.R., Running, S.W., 1997. Estimation of global leaf area index and absorbed PAR using radiative transfer models. *IEEE Trans. Geosci. Remote Sens.* 35 (6), 1380–1393.
- Nemani, R., Running, S.W., 1996. Implementation of a hierarchical global vegetation classification in ecosystem function models. *J. Veg. Sci.* 7, 337–346.
- Nikolov, N., Zeller, K.F., 2003. Modeling coupled interactions of carbon, water and ozone exchange between terrestrial ecosystems and the atmosphere: I. Model description. *Environ. Pollut.* 124, 231–246.
- Nikolov, N.T., Zeller, K.F., 1992. A solar radiation algorithm for ecosystem dynamic models. *Ecol. Model.* 61, 149–168.
- Pielke Sr., R.A., 2001. Influence of the spatial distribution of vegetation and soils on the prediction of cumulus convective rainfall. *Rev. Geophys.* 39, 151–177.
- Pielke, R.A., Avissar, R., Raupach, M., Dolman, A.J., Zeng, X., Denning, A.S., 1998. Interactions between the atmosphere and terrestrial ecosystems: influence on weather and climate. *Global Change Biol.* 4, 461–475.
- Press, W.H., Flannery, B.P., Teukolsky, S.A., Vetterling, W.T., 1988. *Numerical Recipes in C*. Cambridge University Press, New York.
- Privette, J.L., Myneni, R.B., Emery, W.J., Pinty, B., 1995. Inversion of a soil bidirectional reflectance model for use with vegetation reflectance models. *J. Geophys. Res.* 100, 25497–25508.
- Qi, L., Cabot, F., Moran, M.S., Dedieu, G., 1995. Biophysical parameter estimations using multidirectional spectral measurements. *Remote Sens. Environ.* 54, 71–83.
- Ross, J., 1981. *The Radiation Regime and Architecture of Plant Stands*. Dr. W. Junk Publishers, The Hague.
- Sampson, D.A., Smith, F.W., 1993. Influence of canopy architecture on light penetration in lodgepole pine (*Pinus contorta* var. *latifolia*) forests. *Agric. For. Meteorol.* 64, 63–79.
- Scurlock, J.M.O., Asner, G.P., Gower, S.T., 2001. *Worldwide Historical Estimates and Bibliography of Leaf Area Index, 1932–2000* (ORNL Technical Memorandum TM-2001/268). Oak Ridge National Laboratory, Oak Ridge, Tennessee, U.S.A..
- Sellers, P.J., Los, S.O., Tucker, C.J., Justice, C.O., Dazlich, D.A., Collatz, G.J., Randall, D.A., 1996. A revised land surface parameterization (SiB2) for atmospheric GCMs. Part II: The generation of global fields of terrestrial biophysical parameters from satellite data. *J. Clim.* 9, 709–737.
- Tian, Y., Woodcock, C.E., Wang, Y., Privette, J.L., Shabanov, N.V., Zhou, L., Zhang, Y., Buermann, W., Dong, J., Veikkanen, B., Hame, T., Anderson, K., Ozdogan, M., Knyazikhin, Y., Myneni, R.B., 2002a.

- Multiscale analyses and validation of the MODIS LAI product. I. Uncertainty assessment. *Remote Sens. Environ.* 83, 414–430.
- Tian, Y., Woodcock, C.E., Wang, Y., Privette, J.L., Shabanov, N.V., Zhou, L., Zhang, Y., Buermann, W., Dong, J., Veikkanen, B., Hame, T., Anderson, K., Ozdogan, M., Knyazikhin, Y., Myneni, R.B., 2002b. Multiscale analyses and validation of the MODIS LAI product. II. Sampling strategy. *Remote Sens. Environ.* 83, 431–441.
- Wang, Y.P., Jarvis, G.P., 1988. Mean leaf angles for ellipsoidal inclination distribution. *Agric. For. Meteorol.* 43, 319–321.
- Waring, R.H., Landsberg, J.J., Williams, M., 1998. Net primary production of forests: a constant fraction of gross primary production. *Tree Physiol.* 18, 129–134.
- Yang, X., Miller, D.R., 1995. Calculation of potential broadband biologically active and thermal solar radiation above vegetation canopies. *J. Appl. Meteorol.* 34 (4), 861–872.
- Zeller, K., Nikolov, N., 2000. Quantifying simultaneous fluxes of ozone, carbon dioxide and water vapor above a subalpine forest ecosystem. *Environ. Pollut.* 107, 1–20.